

# Photopolymerization of nematic liquid crystal monomers for structural applications: molecular order and orientation dynamics

J.W. Schultz\* and R.P. Chartoff

*The University of Dayton, Center for Basic and Applied Polymer Research, Dayton, OH 45469-0130, USA*

*(Received 14 February 1997)*

This paper is concerned with the molecular orientation in liquid crystal (LC) monomers and the retention of orientation in cross-linked network polymers subsequently formed by photopolymerization. This is of importance because anisotropic mechanical properties can be beneficial in certain structural applications. We have been using LC monomers for forming structural polymers via stereolithography, a novel rapid prototyping process where three-dimensional objects are built layer-by-layer using a laser to scan the surface of a liquid monomer. To this end the magnetic alignment of liquid crystal photo-monomers was investigated with dielectric measurements. Using the permittivity data, an extrapolation method based on the isotropic transition temperature provided an estimate of the order parameter as a function of temperature. The dielectric permittivity was also measured as a function of time after reorientation of an external magnetic field. The calculated change in monomer orientation angle followed an exponential time dependence with two distinct time constants. The faster of the two time regimes was attributed to bulk reorientation and obeyed an Arrhenius type of temperature dependence. The slower time regime was attributed to inhibition caused by impurities and surface interaction with the electrodes. Finally, dynamic mechanical analysis data showed that the molecular anisotropy induced by the magnetic field was retained after polymerization. © 1997 Elsevier Science Ltd.

**(Keywords: liquid crystals; acrylate; dielectric)**

## INTRODUCTION

Because liquid crystals can be oriented, they exhibit anisotropic macroscopic properties. Most research efforts in the past have been concerned with orienting liquid crystals for optical applications (e.g. 'LCD' displays). More recently, however, liquid crystals have found use in mechanical applications. In particular, oriented liquid crystal polymers have anisotropic mechanical properties analogous to composites. Orientation can be induced in thermoplastic liquid crystal polymers by shear forces such as from drawing or extrusion. In thermosets, however, the network locks the molecular order in place, so the alignment must be accomplished before polymerization of the monomer. To align liquid crystal monomers, surface interaction with rubbed substrates is typically used. This technique works well for thin films; however, in applications involving large structural parts, an alternative means of alignment is required to align the bulk of the liquid crystal monomer.

The present work investigates the use of magnetic fields to align liquid crystal monomers prior to polymerization. Once the monomer is aligned, photopolymerization can then be accomplished with a u.v. lamp or laser. This process effectively 'locks-in' the orientation induced by the external magnet because it allows the polymerization to occur while the monomer is still in the liquid crystalline state. Because the magnetic field aligns over much greater distances than rubbed substrates, it can be used to make a wider range of anisotropic parts. One potential application for this is in

stereolithography, which is a commercial technology for rapidly fabricating prototype parts of arbitrary shape from a liquid photo-monomer<sup>1</sup>. In this process three-dimensional objects are formed layer-by-layer as the monomer is photopolymerized using a laser.

Because of the anisotropic mechanical properties that can be achieved, it is possible to engineer specific mechanical properties into structural parts by selectively photopolymerizing different portions under different orientations. To better control the anisotropy in these materials, it is important to have an understanding of how the processing conditions affect the liquid crystal monomer's orientation. Two of these processing variables are temperature and time, and they can have a direct effect on the amount of order in a liquid crystal monomer.

Though the order of a liquid crystal cannot be directly measured, it can be estimated based on the anisotropy of a macroscopic material property. One such material property that is proportional to the amount of molecular order is the dielectric permittivity. The literature contains numerous studies of dielectric behaviour of ordered nematic liquid crystals<sup>2–5</sup>. These works have studied the effect of external magnetic and electric fields on inducing alignment in the nematic phase. While these authors used dielectric anisotropy to qualitatively characterize the alignment, they did not quantitatively estimate the molecular order parameter.

The motivation for the present work is to gain an understanding of the orientation characteristics of reactive liquid crystal resins that can be polymerized into highly cross-linked networks for use in structural applications. In

\*To whom correspondence should be addressed

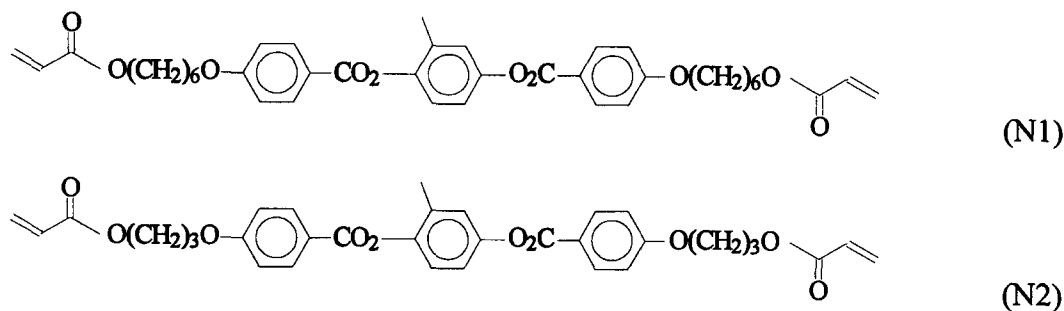


**Figure 1** Molecular structures of the liquid crystal monomers

this work, a dielectric analysis technique has been found to be useful for measuring both the amount of order and the reorientation dynamics of liquid crystal monomers. It is hoped that the results obtained here can be used to better understand how processing conditions affect the formation of liquid crystal photo-polymers.

### EXPERIMENTAL

The liquid crystal monomers used in this study are designated N1 and N2. They are both diacrylate monomers with mesogenic cores made of three aromatic rings linked by ester bridges, and with a methyl group on the central ring. The N1 monomer has 6-carbon aliphatic spacers on each side of the core, while the N2 has 3-carbon spacers. N1 has been studied extensively by Broer *et al.*<sup>6</sup> The molecular structures for N1 and N2 are shown in *Figure 1*.

Both N1 and N2 form a nematic liquid crystalline phase over a wide temperature range. The DSC data shown in *Figure 2* show the melt and crystallization transitions for both of these monomers during a  $5^{\circ}\text{C min}^{-1}$  temperature gradient. As the monomers are heated, they undergo a phase transition from crystalline to liquid crystalline (nematic). Then as they are heated further, they undergo a second-phase transition from nematic liquid crystal to isotropic. Upon cooling, the sequence of events occurs in reverse. An interesting aspect to these data are that while the nematic/isotropic transition is at about the same temperature for both heating and cooling, the crystalline/nematic transition during cooling occurs at a much lower temperature than during heating. This is common in liquid crystal systems and in fact, some liquid crystals exhibit their liquid crystal phase only on cooling. *Figure 2* shows that on cooling, N1 crystallizes to a solid at close to room temperature, while N2 is still a metastable nematic well below room temperature.

For the dielectric measurements, the samples consisted of approximately 250 mg of monomer sandwiched between two parallel gold electrodes, 0.3 mm apart. The permittivity was measured with a Hewlett Packard 4192A impedance analyser using an excitation potential of 1 V. In the frequency range of this instrument (5 Hz to 13 MHz), there was no detectable dipole relaxation so both the permittivity and loss factor curves were relatively flat. The data shown in this paper were taken at 100 kHz.

To orient the LC monomer, a permanent magnet with a field strength of 3200 Oersted across a 10 cm gap was used. The two orientations studied were: (i) with the magnetic field lines parallel to the electric field lines produced between the electrodes; and (ii) with the magnetic field lines perpendicular to the electric field lines. These two orientations are illustrated schematically in *Figure 3*, which shows the orientation of the parallel electrodes with

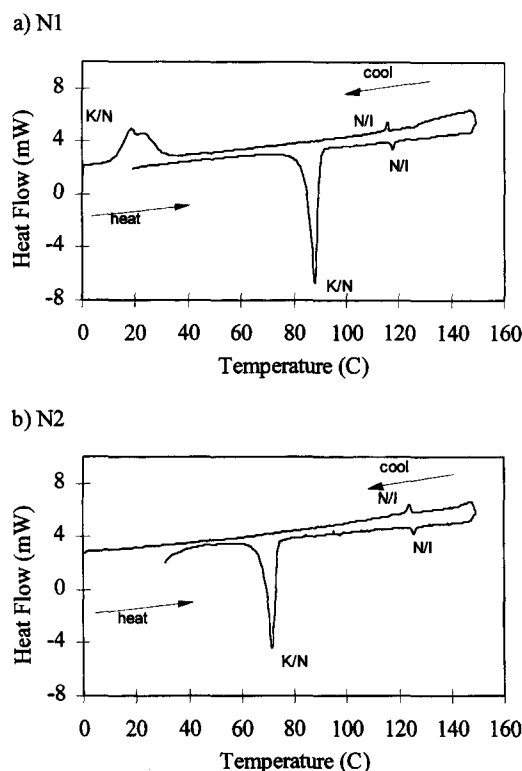


**Figure 2** DSC data showing melt and crystallization transitions for (a) N1 and (b) N2 monomers at a temperature gradient of  $5^{\circ}\text{C min}^{-1}$ . The crystalline/nematic transitions are labelled K/N and the nematic/isotropic transitions are labelled N/I

respect to the magnet poles. Because the liquid crystal is assumed to align parallel to the magnetic field, orientation (i) corresponds to the permittivity parallel to the long axis ( $\epsilon_{\parallel}$ ) and orientation (ii) corresponds to the permittivity perpendicular to the long axis ( $\epsilon_{\perp}$ ).

Besides dielectric studies, some dynamic mechanical measurements were made on polymers of N1 and N2. For photopolymerization, the monomer was mixed with 2% Irgacure 369 (Ciba-Geigy) photoinitiator. To reduce warpage during cure, each sample was mounted with a 0.2 mm teflon spacer between glass slides. The samples were placed in the magnetic field and u.v. cured using an argon ion laser scanned in a raster pattern. During the cure, samples were held at a temperature of  $100^{\circ}\text{C}$ . After the u.v. cure, the samples underwent a thermal postcure at  $230^{\circ}\text{C}$  for 1 h. The dynamic mechanical measurements were conducted on a Rheometrics RSA II, using a thin film fixture. The measurements were made in tension at a frequency of 1 Hz, and a strain of approximately 0.05%. All the samples were heated to  $150^{\circ}\text{C}$  and quickly cooled before testing, to eliminate variations caused by physical aging and internal stresses of the samples.

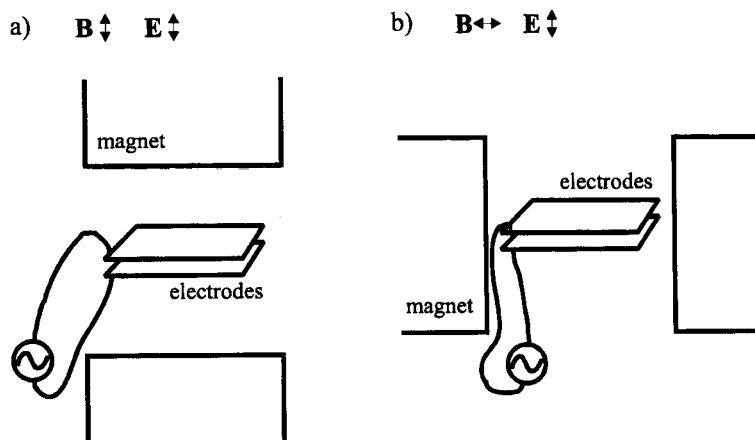


**Figure 3** Experimental set-up of the dielectric measurements. The sample is sandwiched between parallel plate electrodes. An external magnet induces either (a) homeotropic or (b) planar orientation of the LC monomer

## RESULTS AND DISCUSSION

### Order parameter

The temperature variations of the permittivities measured for both  $\epsilon_{\parallel}'$  and  $\epsilon_{\perp}'$ , are shown in *Figure 4(a)* for the N2 monomer, and in *Figure 4(b)* for the N1 monomer. These data also show that at the nematic to isotropic transition temperature, the permittivity anisotropy disappears. Thus, above this transition temperature, there is no longer any long-range molecular order, and the dielectric permittivity is single valued.

To better describe the amount of molecular order in the nematic liquid crystal state, a generally accepted quantity is the molecular order parameter,  $S$ :

$$S = \frac{1}{2} \langle 3\cos^2\theta - 1 \rangle \quad (1)$$

where the brackets indicate that an average is taken over the whole population of molecules. In this equation  $\theta$  is the angle between the main axis of a molecule, and the orientation direction. For a completely ordered material,  $S = 1$ , and for an isotropic material,  $S = 0$ . Extracting the order parameter from dielectric data can be very difficult because of the importance of dipole-dipole interactions between molecules<sup>7</sup>. Maier and Meier<sup>8</sup> derived the following equation for the dielectric anisotropy,  $\Delta\epsilon$ , in a nematic medium:

$$\Delta\epsilon = \frac{NhF}{\epsilon_0} \left( \Delta\alpha - \frac{F\mu^2}{2K_B T} (1 - 3\cos^2\omega) \right) S, \quad (2)$$

where

$$h = \frac{3\bar{\epsilon}}{2\bar{\epsilon} + 1} \text{ and } F = \left( 1 - \frac{2N\bar{\alpha}(\bar{\epsilon} - 1)}{3\epsilon_0(2\bar{\epsilon} + 1)} \right)^{-1}$$

In equation (2),  $N$  is the number of molecules per unit volume,  $\Delta\alpha$  is the molecular polarizability anisotropy,  $\bar{\alpha}$  is the mean polarizability,  $\epsilon_0$  is the dielectric constant of free space,  $\bar{\epsilon}$  is the mean permittivity,  $\mu$  is the permanent dipole moment,  $K_B$  is the Boltzman constant,  $T$  is temperature, and  $\omega$  is the angle between the dipole moment and the principle axis of the molecular polarizability.

If the liquid crystal has little or no dipole moment, the mathematics is greatly simplified. By application of the

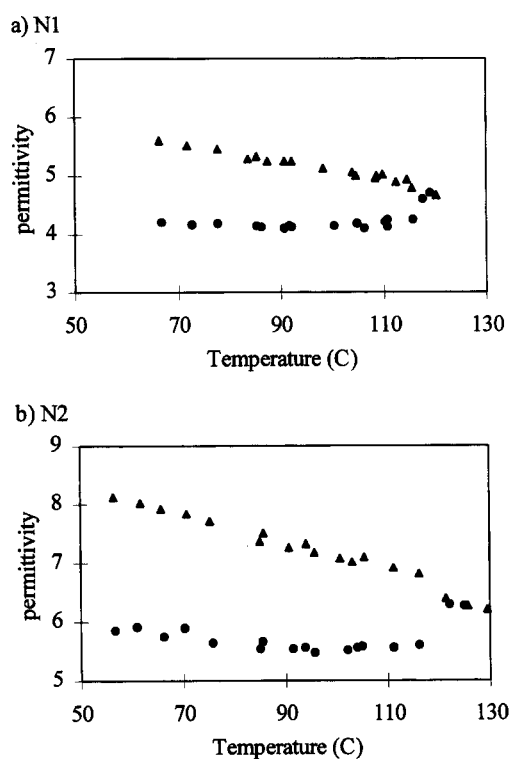


**Figure 4** Plots of measured permittivity as a function of temperature. Both parallel (●) and perpendicular (▲) permittivity data are plotted. Note that when heated beyond the nematic state into the isotropic state, the parallel and perpendicular permittivities become equal

well-known Clausius-Mossotti equation<sup>9</sup>, which relates polarizability to density and permittivity, equation (2) simplifies to

$$S = \left( \frac{\bar{\alpha}}{\Delta\alpha} \right) \left( \frac{\Delta\epsilon'}{\bar{\epsilon}' - 1} \right) \quad (3)$$

equation (3) shows that the order parameter,  $S$ , is directly proportional to the permittivity anisotropy. Normally equation (3) is applied to the index of refraction data measured in optical birefringence experiments. However, because of the lack of dipole relaxation at the dielectric frequencies studied, equation (3) has been extended to the dielectric data in this study. In particular, except for impurity induced electrode blocking effects at the lower frequencies, the permittivity and loss factor of the studied

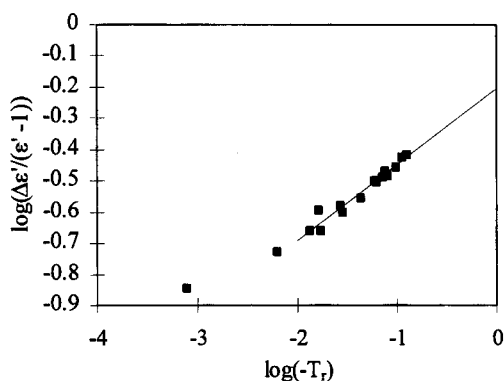


**Figure 5** Plot of  $\log[\Delta\epsilon'/(\bar{\epsilon}' - 1)]$  versus  $\log(-T_r)$  which shows the extrapolation method to estimate the molecular polarizability term for order parameter calculations. The polarizability term is estimated by extrapolating to  $\log(-T_r) = 0$ , and assuming the order parameter is equal to 1 at this point

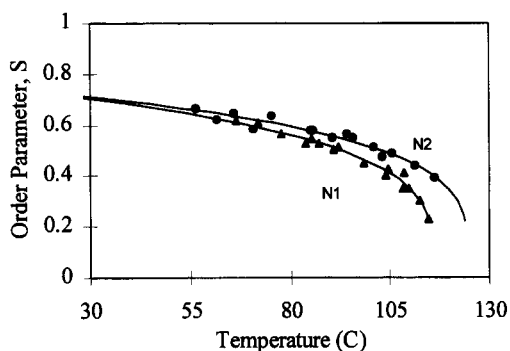


**Figure 6** Estimated order parameter data as a function of temperature. These data are calculated from the measured permittivity data shown in Figure 3. A numerical fit of the data to equation (5) is represented by the solid curves

liquid crystals were essentially flat over the frequency range measured. This is not surprising, given the relatively symmetrical molecular structures shown in Figure 1.

It is important to note that equation (3) also includes molecular polarizability, which cannot be directly measured. To overcome this problem, Haller<sup>10</sup> developed an empirical extrapolation method based on the clearing temperature. In this method, a reduced temperature scale is calculated.

$$T_r = \frac{T - T_{n \rightarrow i}}{T_{n \rightarrow i}} \quad (4)$$

where  $T$  is in Kelvin. A linear dependence between  $\log(\Delta\epsilon'/\bar{\epsilon}' - 1)$  and  $\log(-T_r)$  is assumed, and at absolute zero the liquid crystal is assumed to be perfectly ordered ( $S = 1$ ). Based on equation (3), a linear fit can be extrapolated to estimate  $(\bar{\alpha}/\Delta\alpha)$  from the intercept at  $T_r = -1$  (equivalently,  $\log(-T_r) = 0$ ). This polarizability term,  $(\bar{\alpha}/\Delta\alpha)$  is assumed independent of temperature so that the order parameter can be calculated at the temperatures of interest. An example of this extrapolation is shown in Figure 5.

Figure 6 shows the order parameter calculated from this dielectric data. Broer *et al.* measured the order parameter for the N1 monomer using optical birefringence experiments<sup>6</sup>, and found values 5–10% higher than the data in Figure 6. However, the uncertainty of the extrapolation method may account for this difference. Also shown in

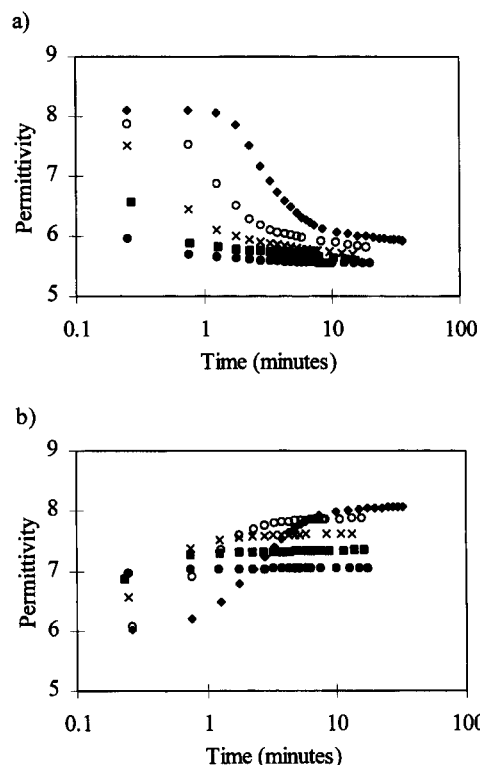


**Figure 7** Summary of measured permittivity data for N2 as a function of time after reorientation of the magnet. For different temperatures, both (a) planar-to-homeotropic and (b) homeotropic-to-planar reorientations show an exponential time dependence:  $\blacklozenge = 50^\circ\text{C}$ ,  $\circ = 60^\circ\text{C}$ ,  $\times = 73^\circ\text{C}$ ,  $\blacksquare = 86^\circ\text{C}$ ,  $\bullet = 100^\circ\text{C}$

Figure 6 are numerical fits of the order parameter data to the equation

$$S = S_0 \left( 1 - \frac{T}{T^*} \right)^f \quad (5)$$

where  $S_0$ ,  $T^*$ , and  $f$  are fitting parameters. This equation was empirically developed by Haller<sup>11</sup>. In more recent work, Magnuson *et al.*<sup>12</sup> showed that this equation follows from a generalization of the Landau–deGennes theory for liquid crystals, and that it successfully describes the temperature dependence of the order parameter over a wide temperature range.

#### Reorientation dynamics

Measurement of the reorientation dynamics was done by quickly rotating the external magnet and measuring the subsequent permittivity as a function of time. A summary of the raw data for N2 at several different temperatures is shown in Figure 7. At time = 0 the magnetic field was quickly removed, then reapplied with a  $90^\circ$  orientation relative to the original field. In Figure 7(a) the magnetic field lines went from perpendicular to parallel with the electric field lines; this corresponds to a reorientation from planar to homeotropic. In Figure 7(b) the magnetic field went from parallel to perpendicular to the electric field; this corresponds to a homeotropic to planar reorientation. The data in these figures show an apparent exponential time dependence.

To gain a better physical understanding of the reorientation dynamics, it is useful to convert this permittivity data into orientation angle data. The orientation angle is modelled by assuming the relative permittivity transforms as a tensor of order two:

$$\epsilon(\theta) = \epsilon_{\parallel} \cos^2 \theta + \epsilon_{\perp} \sin^2 \theta \quad (6)$$

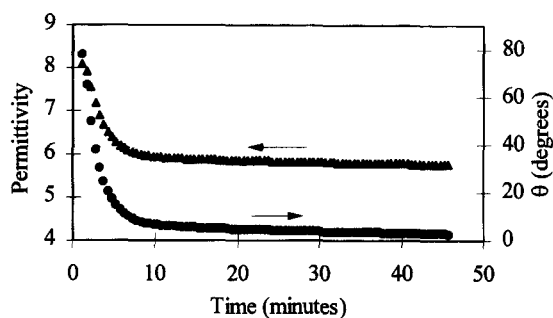


**Figure 8** Permittivity and corresponding orientation angle for N2 at 50°C, when undergoing a planar-to-homeotropic reorientation

Then the orientation angle, relative to its initial value, is given by,

$$\theta = \arccos \left( \frac{\varepsilon(\theta) - \varepsilon(90)}{\varepsilon(0) - \varepsilon(90)} \right) \quad (7)$$

In the analysis of the measured data,  $\varepsilon(0)$  is assumed to be the measured permittivity just before the magnet is rotated. To obtain a value for  $\varepsilon(90)$ , the permittivity at infinite time,  $\varepsilon(\infty)$ , must be estimated. This is not a straight-forward calculation, because the permittivity is always changing, even at long times. For this analysis  $\varepsilon(\infty)$  is estimated by assuming an exponential decay at these long times and doing a non-linear regression of the last few permittivity data points to an offset exponential:

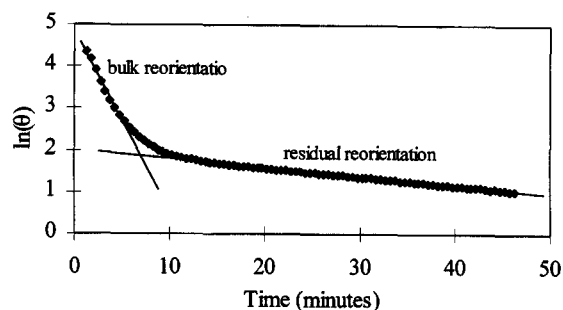
$$\varepsilon(t) = \varepsilon(\infty) + ae^{bt} \quad (8)$$

Figure 8 shows an example of this calculation. The data in this figure are for N2 held at 50°C. Both the raw permittivity values and the corresponding orientation angle values are plotted.

If the orientation angle changes with an exponential time dependence, then a plot of  $\ln(\theta)$  should be linear as a function of time. This is indeed the case, as shown in Figure 9. These data are the same as those of Figure 8. Figure 9 also shows that there are two time regimes in which the liquid crystal relaxes from one orientation to the other. At short times, the permittivity changes with a small time constant, while at long times the permittivity changes with a much larger time constant. It is likely that the initial fast rate of change is due to reorientation of the bulk of the liquid crystals and the secondary slower rate of change is due to reorientation of liquid crystals that are partially bound by surface interaction forces at the electrode interfaces and possibly by impurities. Similar behaviour was observed by Drzaic when he looked at polymer dispersed nematic droplets with optical techniques<sup>13</sup>.

A theoretical basis for reorientation dynamics was first developed by Brochard *et al.*<sup>14,15</sup>. They used the Leslie-Erickson continuum theory of nematic liquid crystals to derive the equations governing reorientation in an infinite slab of nematic. They assumed the nematic was anchored at the top and bottom planes in either a planar or homeotropic configuration. Then, upon application or removal of a magnetic field, they found that there could be both director reorientation and backflow effects, depending on the boundary conditions. When a nematic fluid is first oriented by surface interaction with the substrates, reoriented by a magnetic field and then the field is suddenly removed, the orientation angle follows a simple exponential decay with time:

$$\theta(t) = \theta(0)e^{-t/\tau} \quad (9)$$



**Figure 9** Plot of natural log of the orientation angle for the data of Figure 7. This plot shows two linear regions, corresponding to bulk reorientation and residual reorientation of the liquid crystal monomer

where  $\tau$  depends on the viscosity and elastic constants of the nematic fluid. In the converse case, when a magnetic field is suddenly applied to reorient the nematic fluid, Brochard *et al.* could only develop a theory for small distortions (weak magnetic fields). For the beginning of the reorientation, they found that the orientation angle followed a simple exponential increase. The time constant for this was a function of not only viscosity and elastic constants, but also of the strength of the magnetic field. In geometries where backflow was present, the apparent fluid viscosity was decreased and highly dependent on the magnetic field strength.

In the present study, a slab of nematic fluid also is considered. However, the applied magnetic field is relatively large and the boundary conditions are considerably less ideal. Furthermore, the magnetic field is not removed, as in equation (9), but is instead reapplied 90° from the original field. However, the data shown in Figures 7–9 imply that the exponential law of equation (9) is valid even for the sudden application of large magnetic fields, with non-ideal boundary conditions.

A primary processing variable in the polymerization of these liquid crystal monomers is polymerization temperature. Figure 7 shows that there is a substantial temperature dependence on the reorientation times. A summary of the time constants,  $\tau$ , for the ‘bulk reorientation’ over various temperatures is shown in Figure 10(a). The temperature dependence of this bulk relaxation is quite different from that of the order parameter shown in Figure 6. In fact it follows an Arrhenius type of dependence:

$$\tau = Ae^{B/T} \quad (10)$$

where A and B are constants. By plotting  $\ln \tau$  versus  $1/T$ , a linear behaviour is obtained as shown in Figure 10(b). Thus at temperatures close to the clearing temperature, the nematic reorients very quickly (on the order of seconds), while at lower temperatures the nematic reorientation can slow down to minutes or even tens of minutes. It is likely that the reorientation dynamics also depend on the magnetic field strength; however this was not studied in these experiments.

In addition to the ‘bulk’ reorientation regime, it is also interesting to look at the relaxation phenomenon in the ‘residual’ regime. The residual time constants are plotted Figure 11. These data show that there is an interesting effect that is not seen in the bulk relaxation data. In particular, the data were taken in three different runs, each occurring on a different day. These runs are shown as separate sets of data in Figure 11. As this figure shows, the measured relaxation

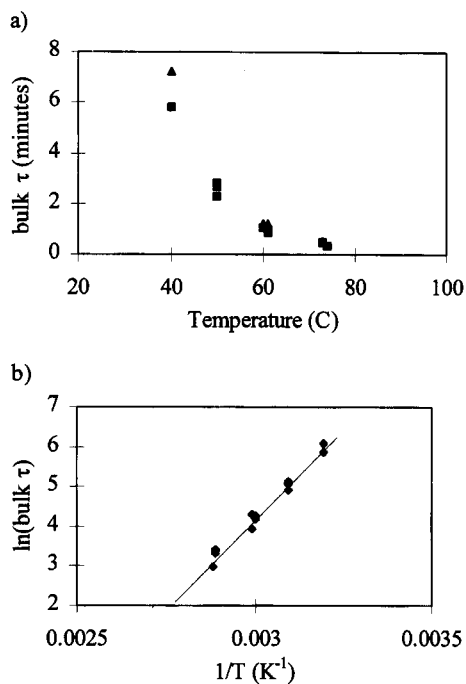


**Figure 10** Temperature dependence of the bulk reorientation time constant. Reorienting from planar-to-homeotropic (▲) and from homeotropic-to-planar (■) both obey the same Arrhenius time dependence, as shown by the straight line in *Figure 10(b)*

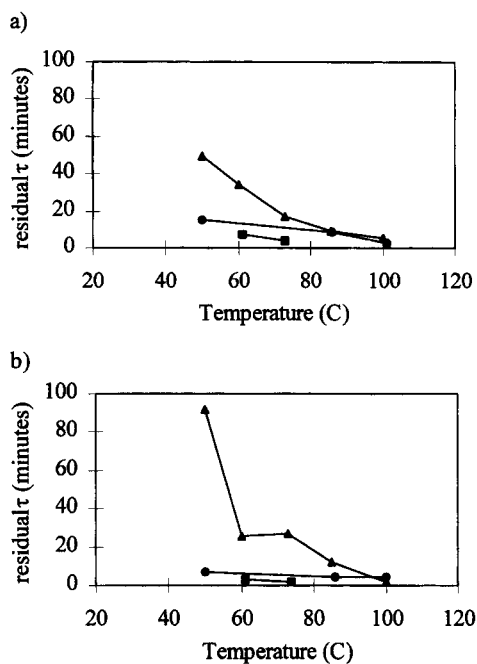


**Figure 11** Temperature dependence of the residual reorientation time constant: (a) planar-to-homeotropic and (b) homeotropic-to-planar reorientation do not have the same time dependence. In addition, data taken on three different days (day 1 = ■, day 2 = ●, day 3 = ▲), show a gradual change in the residual time constants, indicating a physical change in the liquid crystal sample

times increase from the first set of data (day 1) to the last set of data (day 3). If the residual reorientation results from impurities, then this data suggests that the concentration of impurities in the sample increases over time. Thus a likely explanation for this trend is that over a period of hours to days, sufficient polymerization of the monomer (i.e. increase in molecular weight of the polymer impurity)

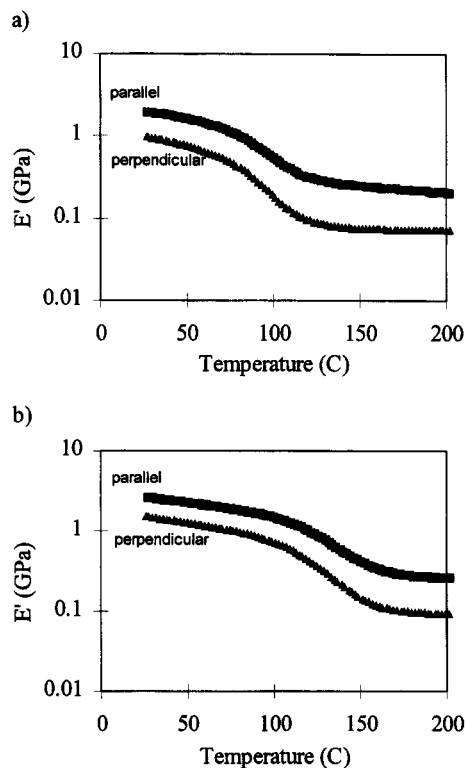


**Figure 12** Dynamic mechanical modulus for (a) polymer N1 and (b) polymer N2. The storage moduli in both the parallel and perpendicular directions is shown

occurs to shift the residual time constants upward. The same upward trend is not seen in the bulk regime shown in *Figure 10*. This is logical, since the bulk nematic phase does not change, only the impurity concentration does. It should be noted that DSC data, not shown here, show a thermal polymerization exotherm beginning at approximately 230°C. However, in a simple polarized microscopy experiment, the monomers were held at a temperature 10–20°C below their isotropic transitions for a period of approximately 6 h. Then after subsequent heating of the monomer into the isotropic state, small regions of material were visible that did not lose their birefringence. This is evidence that a limited amount of polymerization does indeed occur when these monomers are held in the nematic state for long enough periods of time.

*Dynamic mechanical modulus*

The dielectric results show that when the monomer is held at a temperature within its nematic liquid crystalline phase, a magnetic field can be applied to orient the monomer. After waiting an appropriate amount of time for the monomer to fully orient, it can then be photo-polymerized to form a highly cross-linked network with anisotropic mechanical properties. *Figure 12* shows the dynamic storage modulus for both polymers in directions parallel and perpendicular to the orientation. The data of *Figure 12* show that the magnetically induced alignment of the molecules is maintained even after polymerization. Hikmet and Broer<sup>16</sup> have studied the dynamic mechanical modulus of polymer N1 aligned by surface interaction with rubbed substrates, and the values of *Figure 12* agree with their results.

As Hikmet and Broer point out, the modulus anisotropy of these aligned networks is only about a factor of two at room temperature, which is lower than can be achieved in

other main-chain liquid crystal polymers. However, this moderate anisotropy is not surprising given the moderate amount of ordering in the monomer ( $S \sim 0.5-0.6$ ), and the high cross-link density of the polymer. Above the glass transition in the plateau region, the modulus anisotropy is closer to a factor of three. Thus the modulus anisotropy actually increases as the polymer goes through the glass transition.

A possible explanation for the increase of anisotropy, is that the effects of inter-molecular forces decrease as the polymer is heated into the plateau region. As Broer and Mol<sup>17</sup> and Schultz *et al.*<sup>18</sup> have noted, the thermal expansion in the direction perpendicular to alignment is much greater than in the alignment direction. This implies that the change in free volume is also greater in the direction perpendicular to the alignment than in the alignment direction. So, the related anisotropic changes in molecular mobility reflect the diminished effect of inter-molecular forces in a network which is still oriented. Hence, the storage modulus, which is due mainly to the bending and stretching of covalent bonds, decreases more in the direction perpendicular to alignment than in the alignment direction.

## CONCLUSIONS

Dielectric analysis has been used to measure both molecular order and reorientation dynamics in oriented liquid crystal monomers. In this technique, a standard parallel plate geometry was used to measure the permittivity as a function of frequency and temperature. Orientation of the liquid crystal was induced by an external magnetic field.

The molecular order parameter was calculated from the parallel and perpendicular components of the permittivity. Because of the negligible dipole moment in these liquid crystal molecules, the order parameter is directly proportional to the permittivity anisotropy. The proportionality constant was estimated by an extrapolation method. The resulting order parameter values were in reasonable agreement with other values reported in the literature.

The reorientation dynamics were measured by quickly reorienting the magnetic field and measuring the time dependent change in permittivity. These permittivity data were converted into orientation angle values and their time dependence followed an exponential behaviour. Two distinct time regimes were observed. The bulk of the liquid crystal reoriented quickly, while a small amount reoriented with approximately an order of magnitude longer time constant. The reorientation time constants were strongly dependent on temperature. Near the nematic to isotropic transition, the liquid crystal reoriented in a matter of seconds, while at lower temperatures the reorientation time constants were on the order of minutes. The temperature dependence obeyed an Arrhenius type of behaviour. Thus in a processing application where a liquid crystal monomer is oriented, the temperature will have a strong influence on the time it takes for the liquid crystal to reach full orientation. The slower, residual reorientation time was attributed to inhibition by impurities and surface interaction with the electrodes.

Finally, dynamic mechanical analysis showed that the

orientation of the magnetically aligned monomer could be 'locked in' by photopolymerization. The modulus anisotropy for both polymers was approximately a factor of two in the glassy state and a factor of three in the plateau region.

## ACKNOWLEDGEMENTS

The authors are pleased to acknowledge that this research was supported by the US National Science Foundation through NSF grant number DMR-9420357, from the Polymer Program, Division of Materials Research. Doctor Andrew Lovinger was program manager.

## REFERENCES

- Ullett, J.S., Chartoff, R.P., Schultz, J.W., Bhatt, J.C., Dotrong, M. and Pogue, R.T., *Solid Freeform Fabrication Proceedings*, September, 1996, pp. 471-479.
- Carr, E.F., Flint, W.T. and Parker, J.H., *Physical Review A*, 1975, **11**(5), 1732-1736.
- Rao, N.V.S., Kishore, P.R., Raj, T.F.S., Avadhanlu, M.N and Murty, C.R.K., *Molecular Crystallography and Liquid Crystals*, 1976, **36**, 65-73.
- S Rao, N.V., *Molecular Crystallography and Liquid Crystals*, 1984, **108**, 231-243.
- Rondelez, F., Diguët, D. and Durand, G., *Molecular Crystallography and Liquid Crystals*, 1971, **15**, 183-188.
- Broer, D.J., Hikmet, R.A.M. and Challa, G., *Makromolekul Chemika*, 1989, **190**, 3201-3215.
- Vertogen, G. and de Jeu, W.H., *Thermotropic Liquid Crystals, Fundamentals*, Springer, New York, 1988.
- Maier, W. and Meier, G., *Zeitschrift Naturforsch*, 1961, **16A**, 262-267.
- Jackson, J.D., *Classical Electrodynamics*, 2nd edn. Wiley, New York, 1975.
- Haller, I.V., Huggins, H.A., Lilienthal, H.R. and McGuire, T.R., *Journal of Physics and Chemistry*, 1973, **77**(7), 950-954.
- Haller, I.V., *Progress in Solid State Chemistry*, 1975, **10**, 103.
- Magnuson, M.L., Fung, B.M. and Bayle, J.P., *Liquid Crystals*, 1995, **19**(6), 823-832.
- Drzaic, P.S., *Liquid Crystals*, 1988, **3**(11), 1543-1559.
- Brochard, F., Pieranski, P. and Guyon, E., *Physical Review Letters*, 1972, **28**(26), 1681-1683.
- Pieranski, P.F., Brochard, F. and Guyon, E., *Le Journal de Physique*, 1973, **34**(1), 35-48.
- Hikmet, R.A.M. and Broer, D.J., *Polymer*, 1991, **32**(9), 1627-1632.
- Broer, D.J. and Mol, G.N., *Polymer Engineering and Science*, 1991, **31**, 625-631.
- Schultz, J.W., Ullett, J.S., Chartoff, R.P. and Pogue, R.T., *Solid Freeform Fabrication Proceedings*, September 1997.

## Nomenclature

$S$	order parameter
$\theta$	angle
$N$	number of molecules per unit volume
$\Delta\alpha$	molecular polarizability anisotropy
$\bar{\alpha}$	mean polarizability
$\epsilon_0$	dielectric constant of free space
$\bar{\epsilon}$	mean permittivity
$\mu$	permanent dipole moment
$K_B$	Boltzman constant
$T$	temperature
$T_r$	reduced temperature
$\omega$	angle
$S_0, T^*, f, a, b$	numerical fitting parameters
$\tau$	time constant